JGR Space Physics

RESEARCH ARTICLE
10.1029/2021JA030017

Key Points:

- We propose a general curvilinear field-line-following coordinate system which reduces to a usual dipole coordinate system for a dipole field
- Highly accurate results are obtained using the high-order ODE solver to solve the general magnetic field line equations
- Numerical results show that this general curvilinear coordinate system is also an Euler potential or Clebsch type coordinate system

Correspondence to:
H. Wang,
Houjun.Wang@colorado.edu

Citation:
Wang, H. (2022). A General curvilinear magnetic field-line-following coordinate system for ionosphere-plasmasphere modeling. *Journal of Geophysical Research: Space Physics*, *127*, e2021JA030017. https://doi.org/10.1029/2021JA030017

Received 6 OCT 2021
Accepted 19 JAN 2022

A General Curvilinear Magnetic Field-Line-Following Coordinate System for Ionosphere-Plasmasphere Modeling

Houjun Wang[1]

[1]CIRES, University of Colorado at Boulder, Boulder, CO, USA

Abstract We propose a simple way to define a field-line-following, general curvilinear coordinate system for a general magnetic field. This definition of field-line-following coordinate system reduces to a usual definition of dipole coordinate system when the magnetic field is approximated by an axisymmetric dipole. In this way, it can facilitate the numerical implementation by enabling validation of various metric terms computed numerically against those defined analytically in the case of the dipole field. Steps involved in grid generation are also sketched. Highly accurate results are obtained using the high-order ordinary differential equation (ODE) solver to solve the general magnetic field line equations. The accuracy and consistency of the numerical implementation are validated against analytical results in the case of a dipole field. Numerical results show that this field-line-following coordinate system for the general magnetic field, like the coordinates for the dipole field, is also an Euler potential or Clebsch type coordinate system.

1. Introduction

A coordinate system provides a way of organizing data. The kind of coordinate systems to be used depends on the kind of problems to be solved. Because of the fundamental role played by the geomagnetic main fields in plasma motion in ionosphere and plasmasphere, it is often advantageous to organize ionosphere-plasmasphere data or define model variables along magnetic field lines.

Several magnetic coordinate systems have been proposed for ionospheric studies in the past, see Laundal and Richmond (2017) for a comprehensive review. The apex-based coordinates, such as the apex coordinates (VanZandt et al. (1972)), the modified apex coordinates and quasi-dipole coordinates Richmond (1995), were discussed in Emmert et al. (2010), along with the computational aspects of apex-type coordinates. Use of the Euler potentials as coordinate variables is also appealing because of the special properties of the Euler potentials e.g., Stern (1967, 1970).

The Earth's main magnetic field can be best described by the International Geomagnetic Reference Field (IGRF; Thébault et al. (2015)). Approximated magnetic field such as the eccentric dipole, a tilted dipole with an offset center, is sometimes used in the ionospheric modeling (e.g., Bailey et al. (1993); Huba et al. (2000)).

It would be a helpful aid for ionosphere-plasmasphere model development to use the general curvilinear coordinate system that is consistent with conventional mathematical notations. In this paper, we propose and derive a magnetic field-line-following coordinate system that is consistent with the idea and notation of the rigorous mathematics of general curvilinear coordinates. This definition also reduces to a usual definition of the dipole coordinate system in the case of a dipole field.

This paper is organized as follows. In the next section, we present the definition of the general field-line-following coordinate system. Computation of the basis vectors is described in Section 3. Evaluation of numerical implementation and computational results are given in Section 4. And the final section is a summary. Some mathematical details related to algorithm development are presented in the appendices, where grid generation procedures are also briefly described.

2. Definition of Coordinate Systems for the Magnetic Field

2.1. A Coordinate System for the Dipole Magnetic Field

The simplest configuration of a magnetic field is a dipole. To aid our discussion, we start with a definition of a dipole coordinate system. Using the notation of Kageyama et al. (2006), the dipole coordinates (μ, χ, ϕ) for an axial-centered dipole field in terms of the spherical polar coordinates (r, θ, ϕ) are defined as

$$\mu = -\frac{\cos\theta}{r^2}, \quad \chi = \frac{\sin^2\theta}{r}, \quad \phi = \phi, \tag{1}$$

where r is the radial distance from Earth's center, normalized by the geomagnetic conventional Earth's mean reference spherical radius $a = 6{,}371.2$ km, θ the geocentric colatitude, and ϕ the east longitude. The coordinate μ is a magnetic scalar potential function for the dipole field, and the magnetic flux density is given by $\mathbf{B} = -m\nabla\mu$, with m as the dipole moment. The dipole coordinates (μ, χ, ϕ) are *orthogonal*.

It can be shown that

$$\nabla\chi \times \nabla\phi = \nabla\mu. \tag{2}$$

Hence $\mathbf{B} = -m\nabla\mu = -m\nabla\chi \times \nabla\phi$. Thus, the coordinates χ, ϕ are the *Euler potentials* (e.g., Stern, 1970). They are also called the Clebsch-type coordinates (D'haeseleer et al., 1991, Chapter 5).

2.2. A General Curvilinear Magnetic Field-Line-Following Coordinate System

We would like to define a general magnetic field-line-following coordinate system in such a way that, when the magnetic field becomes a dipole, the definition *seamlessly and naturally* becomes the definition of coordinates for a dipole field, the (μ, χ, ϕ) coordinates. Thus, we propose to define a magnetic coordinate system (μ_m, χ_m, ϕ_m) as follows:

$$\mu_m = \hat{\Phi}, \quad \chi_m = \frac{\sin^2\theta_m}{r}, \quad \phi_m = \phi_A, \tag{3}$$

where $\hat{\Phi}$ is a *normalized* magnetic scalar potential (more details later), θ_m is the magnetic colatitude defined by

$$\frac{\sin^2\theta_m}{r} = \frac{1}{r_A}, \tag{4}$$

with r_A the radial distance to the apex (a *constant* for each field line), and ϕ_A is the *geographic* longitude at the apex. Both r_A and ϕ_A are *uniquely* defined for each field line, *as long as each field line has a unique, well-defined apex*. Thus, they can be used to *label* each field line; hence (μ_m, χ_m, ϕ_m) as defined in Eq. (3) can be used as the coordinate variables.

The *normalized* magnetic scalar potential $\hat{\Phi}$ is defined as follows:

$$\hat{\Phi} \equiv \frac{\Phi}{g_m}, \tag{5}$$

where Φ is the magnetic scalar potential and g_m is the dipole moment used here as the normalization factor. The magnetic flux density is then given by $\mathbf{B} \equiv -\nabla\Phi = -g_m\nabla\hat{\Phi} = -g_m\nabla\mu_m$. For the IGRF magnetic field, Φ and g_m are defined in Eqs. (A1) and (A3), respectively.

Remark 1. The differences between the coordinate variables used here and the modified apex coordinates of Richmond (1995) should be noted. As remarked in Emmert et al. (2010), almost all the definition of the apex-like coordinates is motivated by the field line equation for a dipole field, that is, Eq. (B2). In Richmond (1995), modified apex latitude (λ_m) is used as one of the coordinate variables. But the motivation here is to define the general coordinates in *direct* analog to the dipole coordinates. Thus, $\chi_m = 1/r_A$ is used as one of the coordinate variables instead. The magnetic colatitude θ_m can then be defined using Eq. (4), also different from the definition of modified apex latitude (λ_m) of Richmond (1995). (If one chose $r_E + h = r$ in Richmond (1995)'s definition of quasi-dipole latitude λ_q, one would have $\theta_m = \pi/2 - \lambda_q$.) Moreover, the advantage of defining the general coordinates analogous to the dipole coordinates is made explicit here, for example, by using it to verify the implementation of the numerical algorithms in grid generation, see Section 4.

In Richmond (1995), as in VanZandt et al. (1972), the tilted-centered dipole longitude at apex is used as another coordinate variable. The tilted-centered dipole longitude, or simply called the *geomagnetic-dipole longitude* in Richmond (1995), is measured eastward from the meridian half plane bounded by the tilted-centered dipole

axis and containing the south geographic pole (e.g., Fraser-Smith, 1987). Here we simply use the geographic longitude at apex as one of the coordinate variables. This appears to make grid generation easier since the IGRF magnetic field is defined in the geographic/geocentric spherical coordinate system. A grid generation strategy is given in Appendix C. Given the geographic colatitude and longitude at apex, the tilted-centered dipole longitude at apex can be calculated using the IGRF model coefficients; see Appendix C3.

In this work and in Richmond (1995), the magnetic potential, normalized or otherwise, is used as one of the coordinate variables.

Remark 2. More importantly, the definition and computation of basis vectors are done here in more conventional mathematical form, in the same spirit of D'haeseleer et al. (1991). The conventional covariant–contravariant formalism can be seen more in recent works (e.g., Rankin et al., 2006). In contrast, the so-called scaled basis vectors are used in Richmond (1995), involving several scaling factors. This approach appears to be cumbersome, without obvious computational advantage. The desire for using the conventional covariant-contravariant formalism is also expressed in the review paper by Laundal & Richmond (2017, p. 44–45).

Remark 3. Alternative numerical algorithms for grid generation are also introduced, see Appendix C. The high-order ODE solver is used for more accurate and efficient solutions of magnetic field line equations, see Appendix B.

3. Basis Vectors and Metric Terms

Two sets of basis vectors can be defined for a general curvilinear coordinate system. The contravariant-basis vectors are defined as the gradient of the coordinate variables, while the covariant-basis vectors are tangent to the coordinate curves. The two sets of basis vectors are *reciprocal sets of vectors*: One can derive one set of the basis vectors once the other set is known or vice versa (D'haeseleer et al., 1991, Chapter 2).

3.1. Basis Vectors and Metric Terms for a Dipole Field

For a dipole field, the metric terms can be derived analytically. The contravariant-basis vectors are the gradient of the coordinate variables (μ, χ, ϕ), which can be written in terms of the spherical coordinates as.

$$\mathbf{e}^{\mu} \equiv \nabla\mu = \frac{2\cos\theta}{r^3}\hat{\boldsymbol{r}} + \frac{\sin\theta}{r^3}\hat{\boldsymbol{\theta}}, \tag{6a}$$

$$\mathbf{e}^{\chi} \equiv \nabla\chi = -\frac{\sin^2\theta}{r^2}\hat{\boldsymbol{r}} + \frac{2\sin\theta\cos\theta}{r^2}\hat{\boldsymbol{\theta}}, \tag{6b}$$

$$\mathbf{e}^{\phi} \equiv \nabla\phi = \frac{1}{r\sin\theta}\hat{\boldsymbol{\phi}}, \tag{6c}$$

where $\left(\hat{\boldsymbol{r}}, \hat{\boldsymbol{\theta}}, \hat{\boldsymbol{\phi}}\right)$ are unit vectors of the spherical polar coordinates (r, θ, ϕ). The covariant-basis vectors, as the reciprocal of the contravariant-basis vectors, can be computed from the contravariant-basis vectors as follows:

$$\mathbf{e}_{\mu} = \frac{\mathbf{e}^{\chi} \times \mathbf{e}^{\phi}}{\mathbf{e}^{\mu} \cdot (\mathbf{e}^{\chi} \times \mathbf{e}^{\phi})} = \frac{2r^3\cos\theta}{\Theta^2}\hat{\boldsymbol{r}} + \frac{r^3\sin\theta}{\Theta^2}\hat{\boldsymbol{\theta}}, \tag{7a}$$

$$\mathbf{e}_{\chi} = \frac{\mathbf{e}^{\phi} \times \mathbf{e}^{\mu}}{\mathbf{e}^{\chi} \cdot (\mathbf{e}^{\phi} \times \mathbf{e}^{\mu})} = -\frac{r^2}{\Theta^2}\hat{\boldsymbol{r}} + \frac{2r^2}{\Theta^2\tan\theta}\hat{\boldsymbol{\theta}}, \tag{7b}$$

$$\mathbf{e}_{\phi} = \frac{\mathbf{e}^{\mu} \times \mathbf{e}^{\chi}}{\mathbf{e}^{\phi} \cdot (\mathbf{e}^{\mu} \times \mathbf{e}^{\chi})} = r\sin\theta\hat{\boldsymbol{\phi}}, \tag{7c}$$

where Θ is defined as

$$\Theta = \sqrt{1 + 3\cos^2\theta}. \tag{8}$$

The *scale factors* can be computed as

$$h_\mu = |\mathbf{e}_\mu| = 1/|\nabla\mu| = r^3/\Theta, \tag{9a}$$

$$h_\chi = |\mathbf{e}_\chi| = 1/|\nabla\chi| = r^2/(\Theta\sin\theta), \tag{9b}$$

$$h_\phi = |\mathbf{e}_\phi| = 1/|\nabla\phi| = r\sin\theta. \tag{9c}$$

And, in terms of the scale factors, the differential arc length ds is given by

$$ds^2 = ds_\mu^2 + ds_\chi^2 + ds_\phi^2 = (h_\mu d\mu)^2 + \left(h_\chi d\chi\right)^2 + (h_\phi d\phi)^2. \tag{10}$$

For a dipole magnetic field, an analytical expression for the arc length can be obtained, see Eq. (B6). We will compare the arc length computed using Eqs. (B6), (10), and (18) of the general coordinates in the case of a dipole field; see Section 4.1, especially Table 2.

3.2. Basis Vectors and Metric Terms for a General Magnetic Field

For the general magnetic field, the basis vectors and metric terms can only be computed numerically. We first compute contravariant-basis vectors as the gradient of the coordinate variables (e.g., D'haeseleer et al., 1991):

$$\mathbf{e}^i \equiv \nabla u^i. \tag{11}$$

Then, the covariant-basis vectors can be computed from the contravariant-basis vectors as follows:

$$\mathbf{e}_i = \frac{\mathbf{e}^j \times \mathbf{e}^k}{\mathbf{e}^i \cdot (\mathbf{e}^j \times \mathbf{e}^k)}, \tag{12}$$

where i, j and k are chosen such that (i, j, k) forms a cyclic permutation of (1, 2, 3). We will use the correspondence notation $(1, 2, 3) \Leftrightarrow (\mu_m, \chi_m, \phi_m)$.

The computation of $\mathbf{e}^{\chi_m}$ and $\mathbf{e}^{\phi_m}$ are performed in the spherical coordinate system as follows:

$$\mathbf{e}^{\chi_m} \equiv \nabla\chi_m = \frac{\partial\chi_m}{\partial r}\hat{\boldsymbol{r}} + \frac{1}{r}\frac{\partial\chi_m}{\partial\theta}\hat{\boldsymbol{\theta}} + \frac{1}{r\sin\theta}\frac{\partial\chi_m}{\partial\phi}\hat{\boldsymbol{\phi}}, \tag{13}$$

$$\mathbf{e}^{\phi_m} \equiv \nabla\phi_m = \frac{\partial\phi_m}{\partial r}\hat{\boldsymbol{r}} + \frac{1}{r}\frac{\partial\phi_m}{\partial\theta}\hat{\boldsymbol{\theta}} + \frac{1}{r\sin\theta}\frac{\partial\phi_m}{\partial\phi}\hat{\boldsymbol{\phi}}, \tag{14}$$

where the partial derivatives are evaluated using the second-order central difference scheme. Note that the evaluation of the partial derivatives involves tracing along the field line to the apex in order to determine the coordinate values (defined in reference to the apex!) of the neighboring field lines. And that is why an accurate and efficient high-order ODE solver is needed for field line tracing, see Appendix B on solution of field line equations. But the computation of $\mathbf{e}^{\mu_m}$ is done as follows:

$$\mathbf{e}^{\mu_m} \equiv \nabla\mu_m = \nabla\hat{\Phi} = \nabla\Phi/g_m = -\mathbf{B}/g_m, \tag{15}$$

where $\mathbf{B} = B_r\hat{\boldsymbol{r}} + B_\theta\hat{\boldsymbol{\theta}} + B_\phi\hat{\boldsymbol{\phi}}$ is computed using the analytical expressions of Eqs. (A4).

Two important metric coefficients g_{ij} and g^{ij} are defined as

$$g_{ij} = \mathbf{e}_i \cdot \mathbf{e}_j, \quad g^{ij} = \mathbf{e}^i \cdot \mathbf{e}^j. \tag{16}$$

The off-diagonal metric coefficients are all zero for an orthogonal but not necessarily orthonormal coordinate system. The scale factors are defined as $h_i = |\mathbf{e}_i|$. Thus

$$g_{ii} = h_i^2 \quad \text{or} \quad h_i = \sqrt{g_{ii}}, \tag{17}$$

and so h_i's are also called metric coefficients; no summation rule is implied here. Although the h_i's are usually used for orthogonal coordinate systems, the above definition is valid for any coordinate system (D'haeseleer et al., 1991). The arc length can then be computed the same as in the dipole case:

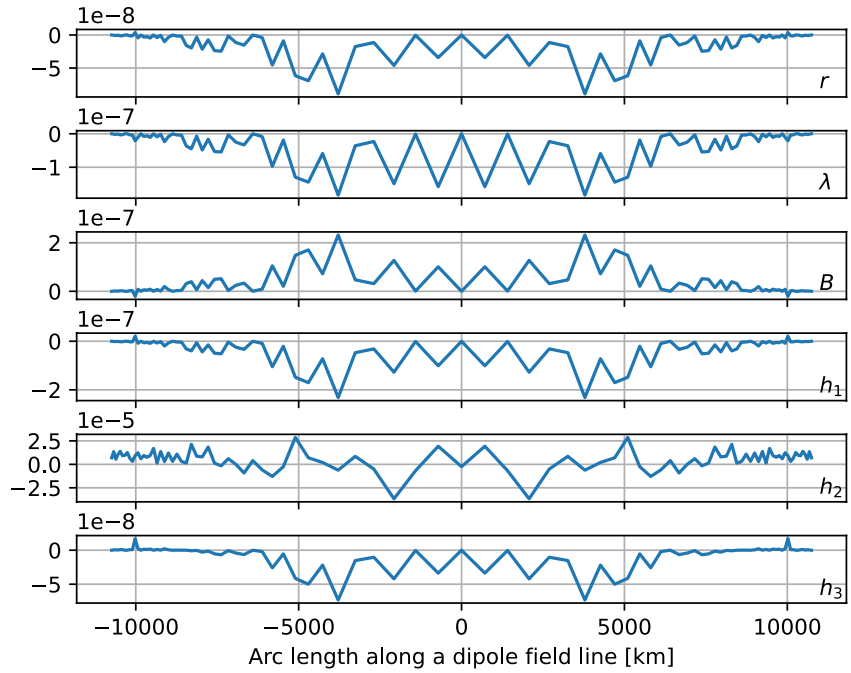

Figure 1. The relative errors of numerically computed spherical coordinate variables (r, λ), magnetic flux density (B), and scale factors (h_1, h_2, h_3) with respect to those computed using analytical expressions in the case of a dipole field line.

$$ds^2 = ds^2_{\mu_m} + ds^2_{\chi_m} + ds^2_{\phi_m} = (h_1 d\mu_m)^2 + (h_2 d\chi_m)^2 + (h_3 d\phi_m)^2, \tag{18}$$

where $h_1 = h_{\mu_m}, h_2 = h_{\chi_m}, h_3 = h_{\phi_m}$, using the correspondence notation $(1, 2, 3) \Leftrightarrow (\mu_m, \chi_m, \phi_m)$.

4. Grid Generation and Computational Results

Grid generation is an important step in ionosphere-plasmasphere model development. It is usually non-trivial, especially for the general magnetic field-line-following coordinates. The procedures of grid generation are briefly described in Appendix C. In this section we evaluate the accuracy of numerical implementation of the algorithms for various coordinate variables and metric terms. In the following presentation, the IGRF-13 coefficients of epoch 2000 are used for the magnetic field, and double precision is used in all numerical computations.

Table 1
The Minima and Maxima of the Relative Errors ε of Spherical Coordinate Variables (r, λ), Magnetic Flux Density (B), and Metric Coefficients (h_1, h_2, h_3) for a Dipole Field Line

ε	Min	Max
R	-8.9068×10^{-8}	3.67×10^{-9}
Λ	-1.8329×10^{-7}	4.93×10^{-12}
B	-2.0742×10^{-8}	2.32×10^{-7}
h_1	-2.3177×10^{-7}	2.08×10^{-8}
h_2	-3.6691×10^{-5}	2.87×10^{-5}
h_3	-7.3187×10^{-8}	1.70×10^{-8}

4.1. Evaluation in the Case of a Dipole Field

Because of the way we define the general coordinate system, we find that the validation of the implementation and the assessment of numerical algorithms can be conveniently performed in the case of a dipole field. This is done as follows:

1. For dipole coordinates, grid generation is done as described in Appendix C1. The basis vectors and metric terms are computed using analytical expressions given in Section 3.1
2. For general coordinates, grid generation is done as described in Appendix C2. Note in choosing/specializing the axial-centered dipole field from the IGRF model, instead of using all the terms as in Eq. (A1), only one term, the g_1^0 term, is used as in Eq. (A2). The basis vectors and metric terms are then computed as described in Section 3.2

Table 2
The Discretized and Continuous Arc Lengths of a Dipole Field Line (s_{gc}, s_{dc}, ℓ) in km and Their Relative Errors ($\varepsilon_{gc/dc}, \varepsilon_{gc/\ell}, \varepsilon_{dc/\ell}$)

K	s_{gc}	s_{dc}	ℓ	$\varepsilon_{gc/dc}$	$\varepsilon_{gc/\ell}$	$\varepsilon_{dc/\ell}$
K51	21,353.9305	21,353.9316	21,355.1369	-4.7904×10^{-8}	-5.6493×10^{-5}	-5.6445 x 10^{-5}
K101	21,480.2391	21,480.2403	21,480.5278	-5.4434×10^{-8}	-1.3438×10^{-5}	$-1.3383\ 10^{-5}$
K201	21,541.8472	21,541.8489	21,541.9191	-7.8555×10^{-8}	-3.3380×10^{-6}	$-3.2595\ 10^{-6}$

Note. The K number denotes different number of points along the field line.

We compare different ways of computing the spherical coordinate variables (radial distance r and latitude $\lambda = \pi/2 - \theta$), magnetic flux density B, and scale factors h_1, h_2 and h_3, for grid points along a dipole field line. We choose the field line crossing the earth's surface at colatitude $\theta = 45°$ at longitude $\phi = 0°$. The field line is divided equally into 101 points in μ, which will be denoted by K101. When computing the gradients in Eq. (15), we use the central finite differences ($\pm\delta r, \pm\delta\theta, \pm\delta\phi$), with step sizes $\delta r = 20$ km, $\delta\theta = 0.25°$, and $\delta\phi = 0.25°$. In the ODE solver for field line equations, the step size is 5 km and error tolerance is 1.00×10^{-12}.

We compute the relative errors of numerically computed values based on the procedure (2) above, relative to their corresponding values based on procedure (1) in the case of axial symmetric dipole field. The relative error $\mathcal{E}_x$ of a variable x is defined as

$$\mathcal{E}_x = (x - x_0)/x_0, \tag{19}$$

where x_0 is the expected value of the variable x. Figure 1 shows the results. They are plotted as the function of the arc length/distance along the field line. First, we notice that these errors are all very small; see also Table 1, which lists the minimum and maximum of these relative errors. Another noticeable feature is that these errors are symmetric about the apex point. This symmetry in the case of the dipole field is a good indicator of the consistency and accuracy of the numerical implementation of the algorithms.

We also calculate the relative errors of different ways of computing the arc length for the field line. We call the arc length calculated using the scale factors from Eqs. (10) and (18) the *discretized arc length*, denoted by s_{dc} and s_{gc}, for dipole coordinates and general coordinates, respectively; while the arc length calculated using the analytical expression Eq. (B6) the *continuous arc length*, denoted by ℓ. Table 2 shows the computed arc lengths [km] of a dipole field line, and their relative errors: w.r.t. s_{dc} ($\varepsilon_{gc/dc}$) or w.r.t. ℓ ($\varepsilon_{gc/\ell}$ and $\varepsilon_{dc/\ell}$). Three different resolutions are shown with K51, K101 and K201 denoting different number of points along the field line. As noted in Appendix C, we use only points above the spherical Earth's surface that satisfy $r \geqslant a + 90$ km; so the arc lengths are different for different resolutions as their end points are not all the same. Again these errors are very small, indicating the high accuracy of the numerical scheme and robustness of the numerical implementation. We also notice the reduction of relative errors w.r.t. ℓ ($\varepsilon_{gc/\ell}$ and $\varepsilon_{dc/\ell}$) as the resolution increases.

Table 3
The Minima and Maxima of the Departures From 90° of the Angles Between the Three Contravariant Basis Vectors in Four Longitudinal Sectors

ϕ_m	β_{12}	β_{13}	β_{23}
0°	-5.8173×10^{-3}	-1.5645×10^{-4}	−5.8443
	4.74×10^{-3}	5.59×10^{-4}	11.0156
90°	-4.4363×10^{-3}	-1.3374×10^{-4}	−9.5587
	5.25×10^{-3}	3.83×10^{-4}	0.6749
180°	-3.9086×10^{-3}	-2.6662×10^{-4}	0.0034
	4.27×10^{-3}	1.75×10^{-4}	3.6654
270°	-3.7511×10^{-3}	-5.2605×10^{-4}	−5.0107
	4.07×10^{-3}	5.72×10^{-4}	6.4699

4.2. Into the General Magnetic Field

For the general magnetic field, two-dimensional grids are generated from the IGRF magnetic field using the grid generation procedure of Appendix C2. The outermost and innermost field lines cross the earth's surface at colatitudes $\theta_m = 45°$ and $\theta_m = 82°$, respectively. They are divided equally into 45 points in χ_m. The resolution along the field lines are determined by dividing the the outermost field line equally into 101 points in μ_m, or K101. Other settings are the same as in the preceding section. Results in four different longitudinal sectors will be presented.

We first check the orthogonality of the coordinates. For this we compute the angles between the contravariant basis vectors. The angles between the three contravariant basis vectors $\mathbf{e}^i$ and $\mathbf{e}^j$, denoted by α_{ij}, can be computed from their dot product

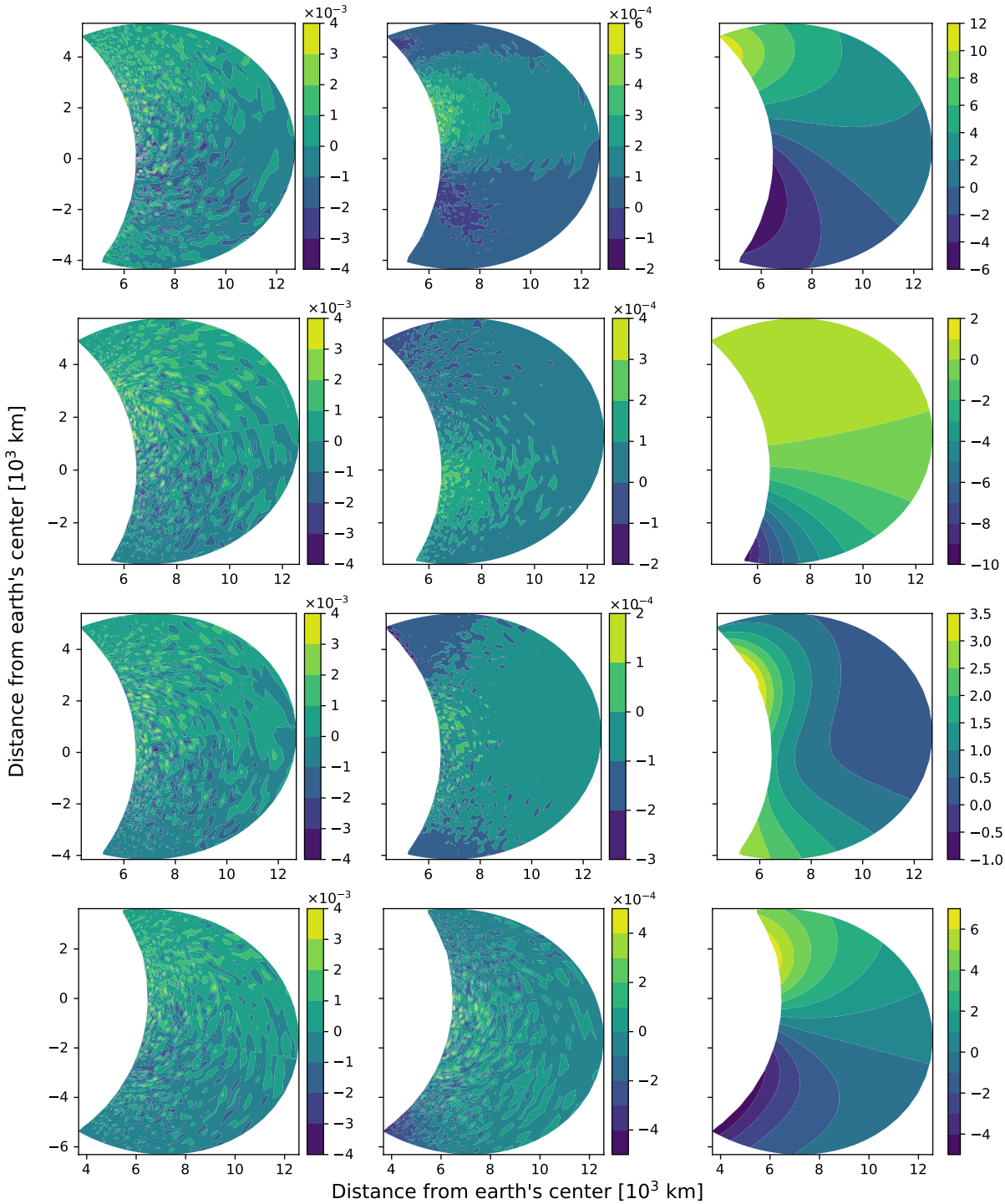

Figure 2. The departures from 90° of the angles between the basis vectors: β_{12} (the 1st column), β_{13} (the 2nd column), and β_{23} (the 3rd column). The four rows are for four longitudinal sectors $\phi_m = 0°$, 90°, 180°, and 270°, respectively.

$$\mathbf{e}^i \cdot \mathbf{e}^j = |\mathbf{e}^i||\mathbf{e}^j|\cos(\alpha_{ij}). \tag{20}$$

The departures from 90° of the angles between the basis vectors

$$\beta_{ij} \equiv \alpha_{ij} - 90°, \tag{21}$$

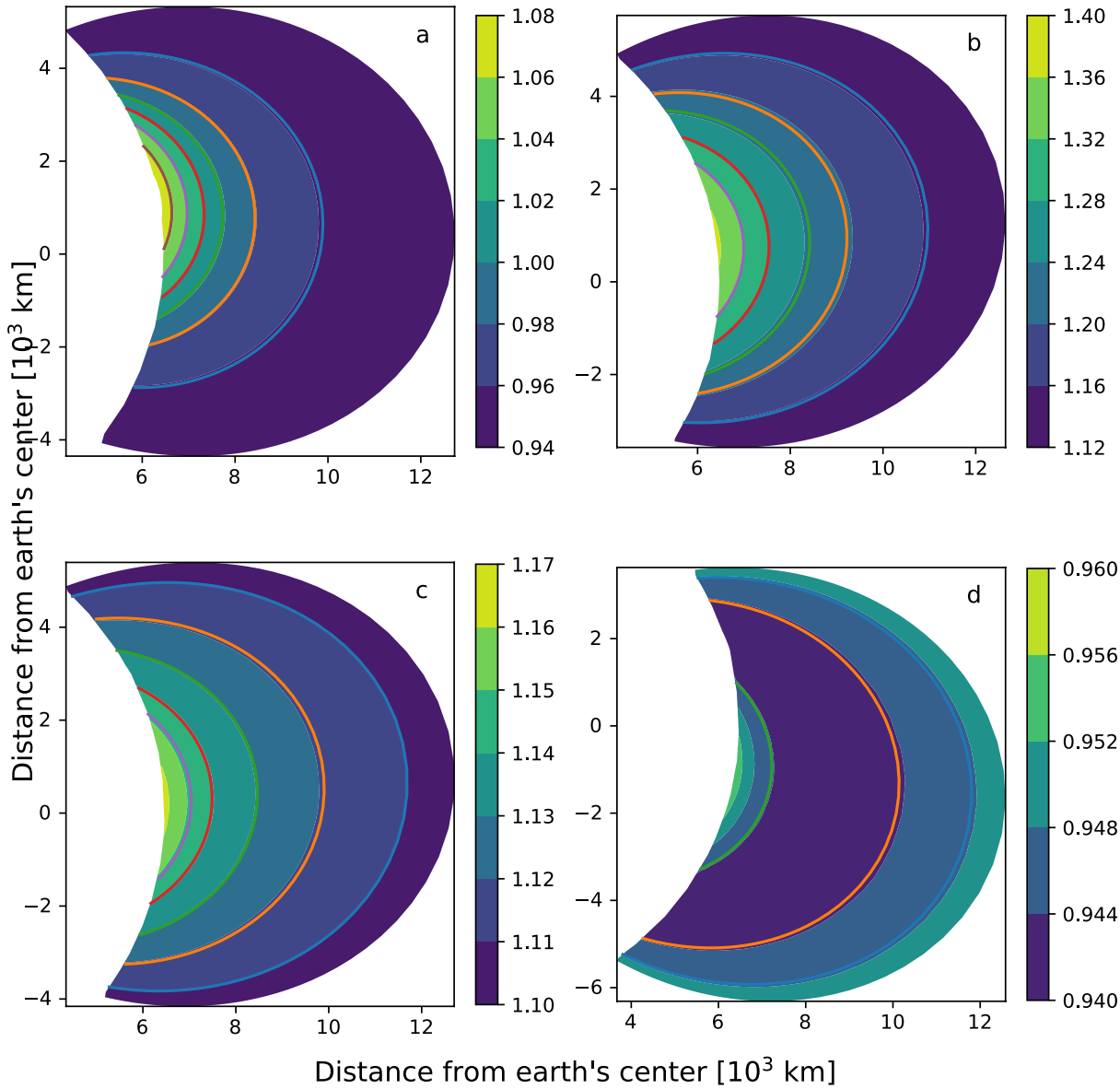

Figure 3. The ratio $\gamma = c/g_m$ in four different longitudinal sectors: (a) $\phi_m = 0°$ with $\gamma_{\min} = 0.9528$, $\gamma_{\max} = 1.0820$, (b) $\phi_m = 90°$ with $\gamma_{\min} = 1.1294$, $\gamma_{\max} = 1.3653$, (c) $\phi_m = 180°$ with $\gamma_{\min} = 1.1054$, $\gamma_{\max} = 1.1624$, and (d) $\phi_m = 270°$ with $\gamma_{\min} = 0.9411$, $\gamma_{\max} = 0.9545$. The color curves are a few selected field lines, illustrating how the contours of ratio γ follow the field lines.

are shown in Figure 2 for four different longitudinal sectors at $\phi_m = 0°$, 90°, 180°, and 270°, respectively. Their minima and maxima are listed in Table 3. They show that both β_{12} and β_{13} are very small. Thus, the two basis vectors $\mathbf{e}^2$ and $\mathbf{e}^3$, though not orthogonal to each other (β_{23} not small), they are both *perpendicular* to $\mathbf{e}^1$, that is, the magnetic field. Here again we use the correspondence notation $(1, 2, 3) \Leftrightarrow (\mu_m, \chi_m, \phi_m)$.

Since both $\mathbf{e}^2$ and $\mathbf{e}^3$ are perpendicular to $\mathbf{e}^1$, their cross product $\mathbf{e}^2 \times \mathbf{e}^3$ would be parallel to $\mathbf{e}^1$, hence also the magnetic field $\mathbf{B}$. Thus, we can write the magnetic field in the following way:

$$\mathbf{B} \equiv -g_m \nabla \mu_m = -c \nabla \chi_m \times \nabla \phi_m, \tag{22}$$

Figure 3 presents the ratio $\gamma = c/g_m$, and a few selected field lines, in four different longitudinal sectors. It shows that the ratio follows the field lines, that is, it is constant along each field line. Thus, the constant c depends only on the field line, and is fixed for each field line. Therefore, χ_m and ϕ_m in the general coordinates, as the

corresponding χ and ϕ in the dipole coordinates, are also Euler potentials. For a dipole field, the ratio $\gamma = c/g_m$ would be a constant 1 everywhere.

The Euler potential, as a potential function, is not uniquely defined. Several different ways to define and construct the Euler potentials have been proposed and used, for example, Stern (1967, 1976, 1994); Ho et al. (1997); Peymirat and Fontaine (1999); Wolf et al. (2006); Rankin et al. (2006). Sometimes the computational procedures can get quite complicated. So depending on the application, the simple approach proposed here may be preferable.

5. Summary

A general curvilinear coordinate system is proposed for ionosphere-plasmasphere modeling. This magnetic field-line-following curvilinear coordinate system reduces to a dipole coordinate system when the magnetic field is a pure dipole.

A high-order ordinary differential equation (ODE) solver is used to solve the magnetic field line equations for the general magnetic field of the IGRF model. The numerical accuracy and consistency of the implementation is validated against the analytical results in the case of a dipole magnetic field. The symmetry of the dipole field can also be used to check the consistency and accuracy of implementation: Any loss of symmetry may indicate loss of accuracy or lack of consistency in the implementation of numerical algorithms.

The general coordinate system is also the Euler potential or Clebsch-type coordinate system. There are infinite choices of Euler potentials for coordinate variables, and it can become complicated sometimes. So depending on the applications, the simple approach used here may be preferred in some cases.

The general curvilinear magnetic field-line-following coordinate system proposed here is developed and implemented while developing a new ionosphere-plasmasphere model. It is also an attempt to put the field-line-following coordinate system on a more rigorous or conventional mathematical framework. Applications of the general coordinates will be presented in a separate paper on ionosphere-plasmasphere modeling (Wang, 2022).

Appendix A: The IGRF Magnetic Field

The Earth's main magnetic field can be best described by the IGRF magnetic field (Thébault et al., 2015; Alken et al., 2021). The magnetic potential Φ of IGRF is approximated by the truncated series, written in the *geocentric spherical coordinates* (r, θ, ϕ), as follows:

$$\Phi(r,\theta,\phi,t) = a\sum_{n=1}^{N}\sum_{m=0}^{n}\left(\frac{a}{r}\right)^{n+1}\left[g_n^m(t)\cos(m\phi) + h_n^m(t)\sin(m\phi)\right]P_n^m(\cos\theta), \tag{A1}$$

where r is the radial distance from the center of the Earth, $a = 6{,}371.2$ km is the geomagnetic conventional Earth's mean reference spherical radius, θ is the geocentric colatitude, and ϕ the east longitude. The functions $P_n^m(\cos\theta)$ are the Schmidt quasi-normalized associated Legendre functions of degree n and order m. The order of approximation is truncated to $N = 10$ for epochs up to 1,995 and $N = 13$ from epoch 2000. In numerical computation of this study, the Schmidt quasi-normalized associated Legendre functions are evaluated using the SHTOOLS (Wieczorek & Meschede, 2018).

The lowest-order approximation, by setting $n = 1$ and $m = 0$ in the truncated series of Eq. (A1), defines an *axial-centered dipole field* (e.g., Bailey et al., 1993):

$$\Phi(r,\theta) = a\left(\frac{a}{r}\right)^2 g_1^0\cos\theta \equiv g_m\left(\frac{a}{r}\right)^2\cos\theta, \tag{A2}$$

where we have defined

$$g_m \equiv a g_1^0 \tag{A3}$$

and may simply be called the *dipole moment*.

The three components of the magnetic field $\mathbf{B} = -\nabla\Phi$ in the spherical coordinates are computed by.

$$B_r = \sum_{n=1}^{N}(n+1)\left(\frac{a}{r}\right)^{n+2}\sum_{m=0}^{n}\left[g_n^m\cos(m\phi) + h_n^m\sin(m\phi)\right]P_n^m(\cos\theta), \tag{A4a}$$

$$B_\theta = \sin\theta\sum_{n=1}^{N}\left(\frac{a}{r}\right)^{n+2}\sum_{m=0}^{n}\left[g_n^m\cos(m\phi) + h_n^m\sin(m\phi)\right]\frac{\partial P_n^m(x)}{\partial x}, \tag{A4b}$$

$$B_\phi = \frac{1}{\sin\theta}\sum_{n=1}^{N}\left(\frac{a}{r}\right)^{n+2}\sum_{m=0}^{n}m\left[g_n^m\sin(m\phi) - h_n^m\cos(m\phi)\right]P_n^m(\cos\theta), \tag{A4c}$$

where we have used

$$\frac{\partial P_n^m(\cos\theta)}{\partial\theta} = -\sin\theta\frac{\partial P_n^m(x)}{\partial x} \tag{A5}$$

by chain rule with $x = \cos\theta$.

Appendix B: Numerical Solution of the Differential Equations for the Magnetic Field Line

B1. The Differential Equations for the Dipole Magnetic Field Line

The differential equations for a dipole field line can be written in the spherical coordinates as

$$\frac{dr}{rd\theta} = \frac{B_r}{B_\theta} = \frac{2\cos\theta}{\sin\theta}. \tag{B1}$$

An analytical expression for the arc length of a dipole field line can be obtained, see for example, (Walt, 1994, pp. 30–31). Integrating the field line equation (B1) gives

$$r = r_A\sin^2\theta, \tag{B2}$$

where r_A is the value of r at apex $\theta = \pi/2$. The arc distance element $d\ell$ along a field line

$$d\ell = \sqrt{(dr)^2 + (rd\theta)^2}, \tag{B3}$$

can be integrated analytically as follows. Differentiating $r = r_A\sin^2\theta$ gives

$$dr = 2r_A\sin\theta\cos\theta\, d\theta. \tag{B4}$$

Thus,

$$\begin{aligned} d\ell &= \sqrt{4r_A^2\sin^2\theta\cos^2\theta + r_A^2\sin^4\theta}\, d\theta \\ &= r_A\sqrt{1+3\cos^2\theta}\sin\theta d\theta. \end{aligned} \tag{B5}$$

Let $x = \cos\theta$, integrating from $x = \cos\theta$ to the equator $x = \cos(\pi/2) = 0$, we get an analytical expression for the arc length of a dipole field line as follows:

$$\ell = \frac{r_A}{2}\left[x\sqrt{1+3x^2} + \frac{1}{\sqrt{3}}\ln\left(\sqrt{1+3x^2} + \sqrt{3}x\right)\right]. \tag{B6}$$

Note that we use ℓ here to distinguish it from the arc length s calculated from the discretized form Eq. (10).

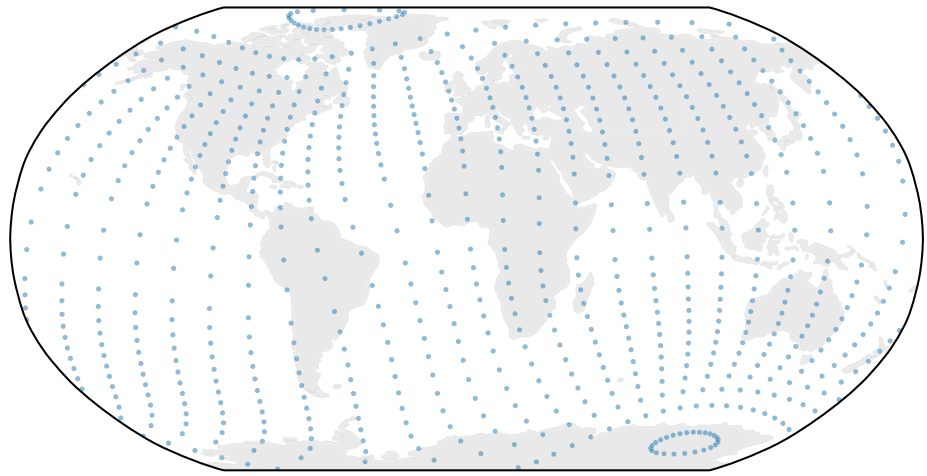

Figure B1. The footpoints of the IGRF field lines on the $r = a$ surface, using 25 longitudinal points and 15 latitudinal points between magnetic colatitudes 5° and 85°.

B2. The Differential Equations for the General Magnetic Field Line

For a general magnetic field such as IGRF, the differential equations for a field line can be written as

$$\frac{\delta s}{B} = \frac{\delta r}{B_r} = \frac{r\delta\theta}{B_\theta} = \frac{r\sin\theta\,\delta\phi}{B_\phi}, \tag{B7}$$

which can be solved for field line (tracing) as follows.

$$r^{n+1} = r^n + \hat{\tau}\left(\frac{B_r}{B}\right)^n (\delta s)^n, \tag{B8a}$$

$$\theta^{n+1} = \theta^n + \hat{\tau}\frac{1}{r^n}\left(\frac{B_\theta}{B}\right)^n (\delta s)^n, \tag{B8b}$$

$$\phi^{n+1} = \phi^n + \hat{\tau}\frac{1}{r^n\sin\theta^n}\left(\frac{B_\phi}{B}\right)^n (\delta s)^n, \tag{B8c}$$

where superscripts n and $n+1$ are position indices; $\hat{\tau} = \hat{\mathbf{s}}\cdot\hat{\boldsymbol{b}} = \pm 1$, with $+$ (or $-$) sign depending on whether $\hat{\mathbf{s}}$ moving/tracing in the same (or opposite) direction of $\hat{\boldsymbol{b}}$ (the unit vector of the magnetic field $\mathbf{B}$).

B3. Numerical Solution of the General Magnetic Field Line Equations

In many applications, such as grid generation described in Appendix C2, accurate and efficient high-order ODE solvers are needed to solve the magnetic field line tracing equations (B8) numerically. In this study, we use the higher-order embedded method, the Runge-Kutta-Fehlberg (RKF45) method. RKF45 is a method of order $O(h^4)$ with an error estimator of order $O(h^5)$, which automatically determines the step-size to achieve the pre-defined accuracy. The RKF45 solver implemented in package rksuite_90 (Brankin & Gladwell, 1997) is used in this study. Highly accurate results are obtained, as shown in Section 4.1 on comparing the numerically computed and the analytically derived results in the case of the dipole field.

Due to singularity at the geographic poles, the values of the magnetic potential and its derivatives at the poles, if needed, are evaluated slightly away from the poles, that is, 5.00×10^{-4} degrees away from the poles. Numerical experiments show that the field line tracing program works near the poles. As an illustration, we use the same grid generation program to trace the IGRF field lines down to the $r = a$ surface. Figure B1 shows the footpoints of the field lines on the surface. However, it should be noted that at higher latitudes (e.g., higher than 85° latitudes), field line tracing can become expensive due to long field lines. Alternative computational strategy, for example, interpolation instead of repeated field line tracing, can be used near the magnetic poles. In addition,

for modeling studies at higher latitudes and higher altitudes, it is also advisable to modify the μ_m coordinate to increase the resolution near the apex. This can be done by a pair of transformations, similar to the dipole coordinate (Kageyama et al., 2006), as follows:

$$\psi_m = \sinh^{-1}(b\mu)/\bar{b}, \tag{B9a}$$

$$\mu_m = \sinh\left(\bar{b}\psi\right)/b, \tag{B9b}$$

where b is parameter controlling the grid distribution along field lines, increasing b leads to the increased resolution near the apex; and $\bar{b} = \sinh^{-1} b$.

Appendix C: Grid Generation for Ionosphere-Plasmasphere Modeling

C1. Grid Generation for Dipole Coordinates

For the dipole coordinates, a uniform grid in (μ, χ, ϕ) with constant ($d\mu$, $d\chi$, $d\phi$) can be generated as follows:

1. Choose two magnetic colatitudes θ_1 and θ_2, where the outermost and innermost field lines intersect with the earth's surface, and a longitude ϕ
2. From the constancy of $\chi = \sin^2\theta/r$ along each field line, find the corresponding radial distances at the magnetic equator, that is, at apex where $\theta = \pi/2$. These are given by $r_{A1} = 1/\sin^2\theta_1$ and $r_{A2} = 1/\sin^2\theta_2$. Grid increment $d\chi$ is determined by dividing $\chi_1 = 1/r_{A1}$ and $\chi_2 = 1/r_{A2}$ into a predefined number of field lines in the meridional plane (ϕ = const.)
3. Grid distribution along the field lines: Grid increment $d\mu$ is determined by dividing the outermost field line equally in μ into K points between the two foot points on the earth's surface, that is, $d\mu = (\mu_A - \mu_1)/((K-1)/2)$, where K is an odd number, $\mu_A = 0$ is the potential at the apex, and $\mu_1 = -\cos(\theta_1)$ is the potential at the foot point on the earth's surface in the northern hemisphere. Grids along the inner field lines are generated using the same grid increment $d\mu$, starting from the apex of each field line. The foot points for each field line are chosen to be the lowest points above the spherical Earth's surface that satisfy for example, $r \geqslant a + 90$ km
4. Compute magnetic flux density, basis vectors, metric terms, scale factors, and the arc length etc

Analytical expressions of the inverse transformation from the dipole coordinates (μ, χ, ϕ) to the spherical coordinates (r, θ, ϕ) are given by Kageyama et al. (2006). These are used in the grid generation for the dipole coordinates.

Note that for the axial-centered dipole coordinates, the geographic/geocentric and magnetic colatitudes are the same, that is, $\theta_m = \theta$. So we do not differentiate between the two in the dipole coordinates.

C2. Grid Generation for General Coordinates

As in defining the general coordinates, which becomes a usual definition of dipole coordinates the field becomes a dipole, grid generation for the general coordinates can be done in a similar way as that for the dipole coordinates.

For the general coordinates, a uniform grid in (μ_m, χ_m, ϕ_m) with constant ($d\mu_m$, $d\chi_m$, $d\phi_m$) can be generated as follows:

1. Choose two magnetic colatitudes θ_{m1} and θ_{m2}, where the outermost and innermost field lines intersect with the earth's surface, and a longitude $\phi_m = \phi_A$, where ϕ_A is the geographic longitude at apex
2. From the constancy of $\chi_m = \sin^2\theta_m/r$ along each field line, find the corresponding radial distances at the magnetic equator, that is, at apex where $\theta_m = \pi/2$. These are given by $r_{A1} = 1/\sin^2\theta_{m1}$ and $r_{A2} = 1/\sin^2\theta_{m2}$. Grid increment $d\chi_m$ is determined by dividing $\chi_{m1} = 1/r_{A1}$ and $\chi_{m2} = 1/r_{A2}$ into a predefined number of field lines in the meridional plane ($\phi_m = \phi_A$ = const.)
3. Grid distribution along the field lines
   a. Find the geographic/geocentric colatitude at apex: Given the geographic coordinates at apex (r_A, ϕ_A) and a first-guess of $\theta'_A = \pi/2$, find θ_A (the geocentric colatitude at apex) using the Newton-Raphson method; and compute the magnetic potential Φ_A at apex. *The apex is defined by $B_r = 0$, thus a turning point.*

b. Tracing down from apex to locate where the field line cross the Earth's surface on both hemispheres, (r_N, θ_N, ϕ_N) and (r_S, θ_S, ϕ_S), and compute the magnetic potentials on both hemispheres, Φ_N and Φ_S, on the Earth's surface.
c. Grid increment $d\mu_m$ along the field lines is determined by dividing the outermost field line equally in μ_m into K points between the two foot points on the earth's surface, that is, $d\mu_m = (\Phi_S - \Phi_N)/g_m/(K-1)$, where g_m is the normalization constant used in the definition of μ_m. Grids along the inner field lines are generated using the same grid increment $d\mu_m$, starting from the apex of each field line. The foot points for each field line are chosen to be the lowest points above the spherical Earth's surface that satisfy for example, $r \geqslant a + 90$ km.

4. Compute magnetic flux density, basis vectors, metric terms, scale factors, and the arc length etc

C3. Computation of the Tilted-Centered Dipole Longitude at Apex

Given the geographic/geocentric colatitude and longitude at apex, (θ_A, ϕ_A), the tilted-centered dipole (TD) longitude at apex can be calculated as follows. The TD are specified by the first three coefficients g_1^0, g_1^1, h_1^1 of the IGRF model. The geographic colatitude and longitude of the north magnetic pole, (θ_N, ϕ_N), are calculated from (Bailey et al., 1993; Fraser-Smith, 1987).

$$\cos\theta_N = -g_1^0/B_0, \tag{C1a}$$

$$\tan\phi_N = h_1^1/g_1^1, \tag{C1b}$$

where $B_0^2 = \left(g_1^0\right)^2 + \left(g_1^1\right)^2 + \left(h_1^1\right)^2$ is a reference magnetic field.

The TD colatitude (ϑ) is measured from the north TD pole and the TD longitude (φ) is measured eastward from the meridian half-plane bounded by the dipole axis and containing the south geographic pole. The TD colatitude and longitude at apex, (ϑ_A, φ_A), are computed from (Bailey et al., 1993; Fraser-Smith, 1987; VanZandt et al., 1972).

$$\vartheta_A = \cos^{-1}\left[\cos\theta_N\cos\theta_A + \sin\theta_N\sin\theta_A\cos\left(\phi_A - \phi_N\right)\right], \tag{C2a}$$

$$\varphi_A = \sin^{-1}\left[\sin\theta_A\sin\left(\phi_A - \phi_N\right)/\sin\vartheta_A\right]. \tag{C2b}$$

We notice that there is a one-to-one correspondence between (θ_A, ϕ_A) and (ϑ_A, φ_A). Numerical experiments show that if φ_A is used as one coordinate variable in place of ϕ_A, the nice properties of the angles between basis vectors and the ratio γ for Euler potentials are still maintained. This is understandable as it is just a different way of *labeling* the field line. But caution should be exercised when interpolating model results or coupling with other models that use the geomagnetic-dipole longitude as the longitude coordinate. And the geographic/geocentric spherical coordinates are the bases of all other coordinate systems.

Data Availability Statement

Data available at https://doi.org/10.5281/zenodo.5768675.

Acknowledgments
Thanks to the reviewers for their careful reading and constructive comments that helped to clarify and improve the presentation.

References

Alken, P., Thébault, E., Beggan, C. D., Amit, H., Aubert, J., Baerenzung, J., & Zhou, B. (2021). International geomagnetic reference field: The thirteenth generation. *Earth Planets and Space*, *73*(1), 1–25. https://doi.org/10.1186/s40623-020-01288-x

Bailey, G. J., Sellek, R., & Rippeth, Y. (1993). A modelling study of the equatorial topside ionosphere. *Annales geophysicae*, *11*, 263–272.

Brankin, R. W., & Gladwell, I. (1997). Algorithm 771: Rksuite_90: Fortran 90 software for ordinary differential equation initial-value problems. *ACM Transactions on Mathematical Software*, *23*(3), 402–415. https://doi.org/10.1145/275323.275328

D'haeseleer, W. D., Hitchon, W. N. G., Callen, J. D., & Shohet, J. L. (1991). *Flux coordinates and magnetic field structure*. Springer-Verlag.

Emmert, J. T., Richmond, A. D., & Drob, D. P. (2010). A computationally compact representation of Magnetic-Apex and Quasi-Dipole coordinates with smooth base vectors. *Journal of Geophysical Research*, *115*(A8), A08322. https://doi.org/10.1029/2010JA015326

Fraser-Smith, A. C. (1987). *Centered and eccentric geomagnetic dipoles and their poles*, 1600–1985 (Vol. 25) (No. 1). https://doi.org/10.1029/RG025i001p00001

Ho, C. W., Huang, T. S., & Gao, S. (1997). Contributions of the high-degree multipoles of Neptune's magnetic field: An Euler potentials approach. *Journal of Geophysical Research*, *102*(A11), 24393–24401. https://doi.org/10.1029/97JA01649

Huba, J. D., Joyce, G., & Fedder, J. A. (2000). Sami2 is Another Model of the Ionosphere (SAMI2): A new low-latitude ionosphere model. *Journal of Geophysical Research*, *105*(A10), 23035–23053. https://doi.org/10.1029/2000JA000035

Kageyama, A., Sugiyama, T., Watanabe, K., & Sato, T. (2006). A note on the dipole coordinates. *Computers & geosciences*, *32*(2), 265–269. https://doi.org/10.1016/j.cageo.2005.06.006

Laundal, K. M., & Richmond, A. D. (2017). Magnetic coordinate systems. *Space Science Reviews*, *206*(1–4), 27–59. https://doi.org/10.1007/s11214-016-0275-y

Peymirat, C. & Fontaine, D. (1999). A numerical method to compute Euler potentials for non dipolar magnetic fields. *Annales geophysicae*, *17*(3), 328–337. https://doi.org/10.1007/s00585-999-0328-6

Rankin, R., Kabin, K., & Marchand, R. (2006). Alfvénic field line resonances in arbitrary magnetic field topology. *Advances in Space Research*, *38*(8), 1720–1729. https://doi.org/10.1016/j.asr.2005.09.034

Richmond, A. D. (1995). Ionospheric electrodynamics using magnetic apex coordinates. *Journal of Geomagnetism and Geoelectricity*, *47*(2), 191–212. https://doi.org/10.5636/jgg.47.191

Stern, D. P. (1967). Geomagnetic Euler potentials. *Journal of Geophysical Research*, *72*(15), 3995–4005. https://doi.org/10.1029/JZ072i015p03995

Stern, D. P. (1970). Euler potentials. *American Journal of Physics*, *38*(4), 494–501. https://doi.org/10.1119/1.1976373

Stern, D. P. (1976). Representation of magnetic fields in space. *Reviews of Geophysics*, *14*(2), 199–214. https://doi.org/10.1029/RG014i002p00199

Stern, D. P. (1994). Euler potentials of current-free fields expressed in spherical harmonics. *Journal of Geophysical Research*, *99*(A2), 2443. https://doi.org/10.1029/93ja03168

Thébault, E., Finlay, C. C., Beggan, C. D., Alken, P., Aubert, J., Barrois, O., & Zvereva, T. (2015). International geomagnetic reference field: The 12th generation. *Earth Planets and Space*, *67*(1), 79. https://doi.org/10.1186/s40623-015-0228-9

VanZandt, T. E., Clark, W. L., & Warnock, J. M. (1972). Magnetic apex coordinates: A magnetic coordinate system for the ionospheric F2 layer. *Journal of Geophysical Research*, *77*(13), 2406–2411. https://doi.org/10.1029/JA077i013p02406

Walt, M. (1994). *Introduction to geomagnetically trapped radiation*. Cambridge University Press. https://doi.org/10.1017/CBO9780511524981

Wang, H. (2022). Development of a discontinuous Galerkin ionosphere-plasmasphere model. *Journal of Geophysical Research: Space Physics*. https://doi.org/10.1029/2021ja030047

Wieczorek, M. A., & Meschede, M. (2018). SHTools: Tools for working with spherical harmonics. *Geochemistry, Geophysics, Geosystems*, *19*(8), 2574–2592. https://doi.org/10.1029/2018GC007529

Wolf, R. A., Spiro, R. W., Sazykin, S., Toffoletto, F. R., Le Sager, P., & Huang, T.-S. (2006). Use of Euler potentials for describing magneto-sphere-ionosphere coupling. *Journal of Geophysical Research*, *111*(A7), A07315. https://doi.org/10.1029/2005JA011558